AIP | Applied Physics Letters

In adlayer mediated molecular beam epitaxial growth and properties of a -plane InN on freestanding GaN

G. Koblmüller, G. D. Metcalfe, M. Wraback, F. Wu, C. S. Gallinat, and J. S. Speck

Citation: Applied Physics Letters **94**, 091905 (2009); doi: 10.1063/1.3092482
View online: http://dx.doi.org/10.1063/1.3092482
View Table of Contents: http://scitation.aip.org/content/aip/journal/apl/94/9?ver=pdfcov
Published by the AIP Publishing

In adlayer mediated molecular beam epitaxial growth and properties of *a*-plane InN on freestanding GaN

G. Koblmüller,[1,a)] G. D. Metcalfe,[2] M. Wraback,[2] F. Wu,[1] C. S. Gallinat,[1] and J. S. Speck[1]
[1]*Materials Department, University of California, Santa Barbara, California 93106, USA*
[2]*Sensors and Electron Devices Directorate, U.S. Army Research Laboratory, Maryland 20783, USA*

(Received 4 February 2009; accepted 5 February 2009; published online 4 March 2009)

The role of the In adlayer on the morphological and structural properties of nonpolar *a*-plane InN films was elucidated during the plasma-assisted molecular beam epitaxy on freestanding GaN. Reflection high energy electron diffraction during In adsorption experiments on *a*-plane InN surfaces revealed a stable In adlayer coverage of ~2 ML. This In adlayer-mediated growth was responsible for achieving atomically smooth surfaces (rms roughness of <1 nm), phase-pure material with lower x-ray rocking curve widths ($\Delta\omega<0.5°$), lower crystal mosaic tilt/twist, and decreased stacking fault densities, compared to N-rich conditions. The photoluminescence peak emission and band gap energy of the *a*-plane InN films were ~0.63 and ~0.7 eV, respectively. © *2009 American Institute of Physics*. [DOI: 10.1063/1.3092482]

Despite intense efforts to enhance many physical properties of indium nitride (InN), this underdeveloped group-III nitride material has found relatively few applications in devices. These limitations are in part caused by an electron accumulation layer at the InN surface due to surface Fermi level pinning in the conduction band,[1] restricting the fabrication of *p*-type InN layers.[2] To facilitate pure *p*-type InN and drive research toward device applications, first-principle calculations[3] suggested that growth along nonpolar, i.e., the *a*-plane ($[11\bar{2}0]$) and *m*-plane ($[1\bar{1}00]$) orientations, would yield surfaces without an accumulation layer. However, this was proposed only for reconstructed nonpolar InN surfaces without metal adlayers or In–In bonding states in the conduction band. The absence of electron accumulation on nonpolar InN surfaces was recently demonstrated, indeed, on *in situ* cleaved *a*-plane InN,[4] but not on as-grown surfaces, due to nonhomogeneous, highly defective surfaces[5,6] and metal In coverage,[7] which contributed to *n*-type surface states in both *a*- and *m*-plane InN.

So far, all *a*-plane InN films were grown on *r*-plane ($[1\bar{1}02]$) sapphire, which suffered from cubic inclusions,[8] three-dimensional (3D) growth mode,[5] surface roughness >50 nm (Ref. 9) and poor electronic transport (electron mobilities at <250 $cm^2/V\,s$),[5] pointing to apparent difficulties in fabricating high-quality nonpolar InN. More recently though, the first step toward phase-pure nonpolar InN films with smooth surfaces was achieved for the *m*-plane, owing to the availability of high-quality freestanding *m*-plane GaN substrates and knowledge of thermal dissociation.[10]

To establish *a*-plane InN films with similar qualities and understand the critical In adlayer issues, we report in this letter on the influence of the In adlayer kinetics during the plasma-assisted molecular beam epitaxy (PAMBE) on the surface and structural properties of the *a*-plane InN. Specifically, under In-rich conditions, In-adlayer-mediated growth was found to enhance the surface diffusion, the film mosaic, and the basal-plane stacking fault densities, surpassing previous problems associated with *a*-plane InN films.

As substrate material, on-axis *a*-plane freestanding GaN (Mitsubishi Chemical Co.) was used, which was sliced from a bulk GaN crystal along its *c*-direction. The *a*-plane InN films were grown in a Varian Gen-II MBE system, equipped with standard effusion cells for In and Ga. Active nitrogen was supplied by a Veeco Unibulb radio-frequency plasma source, using a N_2 flow rate of 0.4 sccm and plasma power of 300 W (i.e., equivalent to N limited growth rate of ~6 nm/min). To produce low-impurity InN/GaN interfaces, the *a*-plane GaN substrates were overgrown with ~50 nm of MBE-GaN under Ga-rich conditions.

First, the onset for thermal dissociation was determined by recording the reflection high-energy electron diffraction (RHEED) intensity during the growth of ~10 min long InN pulses under variable temperatures ($T=380-500$ °C) at constant N-rich conditions (In/N=0.8).[10] As typical for N-rich group-III nitride growth,[11] these pulses produced spotty RHEED patterns, however, only up to $T\sim430$ °C. Higher temperatures resulted in very low-contrast RHEED patterns due to the large In droplets accumulating on the surface as a result of thermal dissociation.[12] Thus, ~430 °C was the practical onset temperature for thermal dissociation, being nearly identical to that for *m*-plane InN,[10] but much lower than the dissociation temperature reported for *c*-plane InN.[13,14]

We selected therefore $T=420$ °C as the maximum growth temperature and further analyzed the effect of the In/N flux ratio on the surface morphology. The atomic force micrographs in Fig. 1 show surfaces of three *a*-plane InN films grown under different In/N flux ratios, i.e., (a)=0.6 (N-rich growth), (b)=1 (flux stoichiometry), and (c)=1.25 (In-rich growth). The film thicknesses varied between (a)

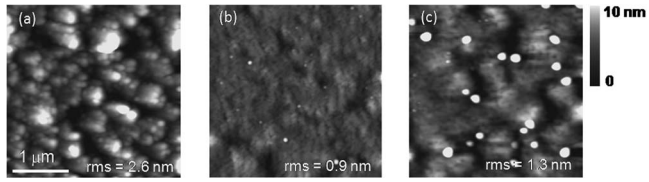

FIG. 1. 3×3 μm^2 AFM images of *a*-plane InN grown on freestanding GaN at constant $T=420$ °C, but variable In/N flux ratio: (a) In/N=0.6, (b) In/N=1, and (c) In/N=1.25.

a)Author to whom correspondence should be addressed. Electronic mail: Gregor.Koblmueller@wsi.tum.de.

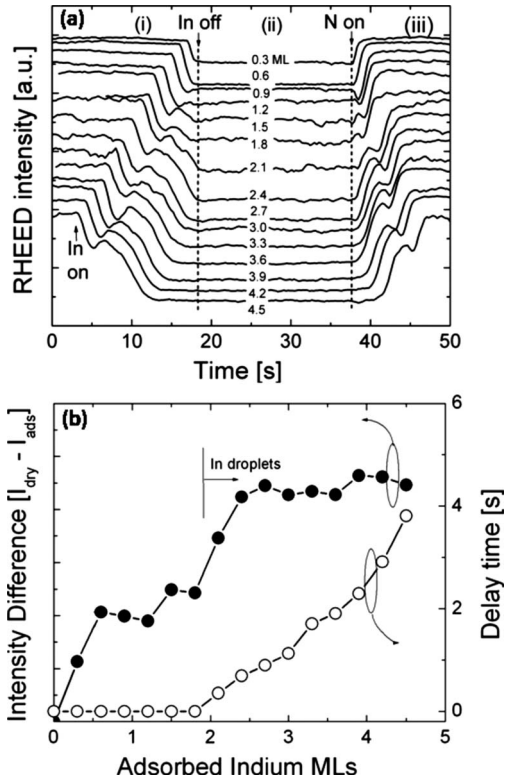

FIG. 2. (a) RHEED intensity profiles during the adsorption of different In coverages and their consecutive consumption by active N on *a*-plane InN surfaces. Note that pronounced oscillatory transients indicated a saturated In-adlayer coverage of 2 ML. (b) Further evidence of the 2 ML thick In-adlayer shown by the saturation in RHEED intensity difference (determined from intensity levels between nitridated and In-adlayer-stabilized surfaces) and the In-droplet related delay in the oscillation onset for In >2 ML.

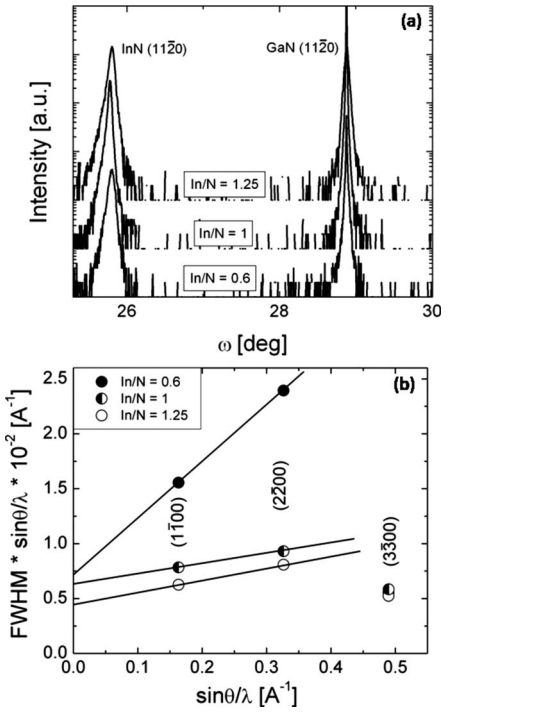

FIG. 3. (a) ω-2θ XRD scans of *a*-plane InN films grown on *a*-plane free-standing GaN under different In/N flux ratios (0.6–1.25). (b) WH plots of the BPSF sensitive reflections in the *m*-plane scattering plane and in skew symmetry for the same three InN films, giving the mosaic tilt/twist by the fitted slope angles and the BPSF density from the intercept with the ordinate.

300 nm, (b) 900 nm, and (c) 500 nm, respectively. Obviously, N-rich conditions yielded highly facetted 3D surfaces with rms ~2.6 nm (over 3×3 μm^2). Crossing flux stoichiometry toward more In-rich conditions reduced the 3D features and decreased the rms roughness to ~1 nm. The dots visible in Fig. 3(c) represent In droplets.

M-plane InN surfaces showed striated morphologies along the *a*-direction that were associated with the intersection of basal plane stacking faults with the surface.[10,15–17] Such striations were absent on the *a*-plane InN surfaces, as was the case for *a*-plane GaN.[18] This low morphological anisotropy could be attributed to similar adatom diffusion energies along the in-plane *c*- and *m*-directions on *a*-plane surfaces, compared to the more different energies along the *c*- and *a*-directions calculated for *m*-plane surfaces.[19]

To explain the much smoother morphologies for films grown above flux stoichiometry (In/N $\geq$ 1), we proposed a stable In adlayer at the growth surface that enhances the surface diffusion. This In adlayer and its maximum coverage on the *a*-plane InN was identified via specific RHEED intensity measurements. By adsorbing variable In coverages (0.3–4.5 ML) onto a nitridated InN surface and subsequently consuming these by InN growth with active nitrogen (all at a fixed T=400 °C), various different RHEED intensity curves were observed [Fig. 2(a)]. Note that 1 ML of In corresponds to the unit cell height of the *a*-plane InN, i.e., $a^{InN}/2$ =1.77 Å.

Three different regimes were characterized: (i) drop in intensity upon In adsorption due to the formation of the In adlayer, (ii) constant intensity after closing the In shutter (In-adlayer stabilized surface), and (iii) rise in intensity during the consumption of the In adlayer by an active N, resulting in the initially nitridated surface. Also, with increasing In adsorption time (duration between "In on" and "In off") different oscillatory transients were observed, depending on the amount of adsorbed In. For In coverages below 1 ML, barely any oscillatory transients were found, while for 1 ML $<$ In <2 ML, clear oscillatory transients appeared.

For In coverages >2 ML there was a gradual delay in the onset of the oscillatory transient upon N consumption [Fig. 2(b)], indicating that In droplets formed. In addition, plotting the difference in the RHEED intensity between the fully nitridated and In-adlayer stabilized surface, we observed a steady increase with rising In coverage until saturation occurred for In coverages of $\geq$2 ML [Fig. 2(b)]. From all these observations we can clearly state that the maximum In adlayer coverage on *a*-plane InN amounts to ~2 ML, similar to the reported In adlayer coverage on *c*-plane InN.[20]

The role of the In adlayer on the structural properties was analyzed by high-resolution x-ray diffraction, shown by

TABLE I. Measured values of XRD rocking curve widths from (11$\bar{2}$0) ω scans along both the in-plane *c*- and *m*-orientations; the corresponding film mosaic tilt/twist $\Delta\omega$ (skew) and BPSF densities from WH analysis for the three investigated *a*-plane InN films.

	$\Delta\omega$(11$\bar{2}$0)			
In/N	*m* (deg)	*c* (deg)	$\Delta\omega$ (skew) (deg)	ρ (SF) (cm^{-1})
0.6	0.62	0.68	2.94	1.5×10^6
1	0.54	0.63	0.51	1.2×10^6
1.25	0.49	0.56	0.64	8.8×10^5

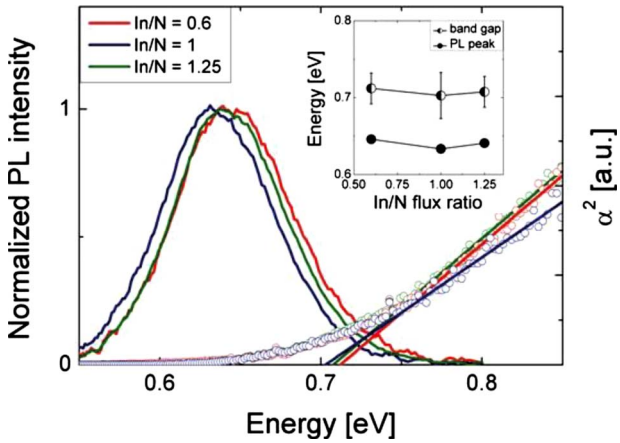

FIG. 4. (Color online) Room temperature PL and optical absorption spectra for the three selected *a*-plane InN films grown at T=420 °C and varying In/N flux ratios. The band gap energy was determined by the intercept of the linear fits of the square of the absorption coefficient with the energy axis.

the $(11\bar{2}0)$ ω-2θ scans of the three *a*-plane InN films grown under the different In/N flux ratios in Fig. 3(a). For all films, two single diffraction peaks were identified, associated with the *a*-plane InN film and the *a*-plane GaN substrate. We also measured the $(11\bar{2}0)$ rocking curve widths [full width at half maximum (FWHM) of ω scans] for the two orthogonal in-plane *c*-([0001]) and *m*-($[1\bar{1}00]$) orientations, as listed in Table I. Two main trends were found: (i) A gradual decrease in FWHMs with increasing In/N flux ratio for both orientations, and (ii) slightly lower FWHMs along the *m*-orientation, although this deviation was not too significant due to the similar adatom diffusion[19] and low morphological anisotropy along the two orthogonal in-plane orientations.

The FWHMs of ω scans contain contributions by the basal-plane stacking faults (BPSFs), which can be separated by Williamson–Hall (WH) analysis.[21,22] However, both the accessible on-axis reflections of the *a*-plane InN, i.e., $(11\bar{2}0)$ and $(22\bar{4}0)$, were found insensitive to the BPSFs and the derived FWHMs would yield only the mosaic tilt.[23,24] Determining the BPSFs, we focused on the BPSF sensitive reflections $(1\bar{1}00)$ and $(2\bar{2}00)$ (within the *m*-scattering plane), being readily accessible in skew symmetry (ψ=30°).[24]

The FWHMs of these BPSF sensitive reflections $(1\bar{1}00)$ and $(2\bar{2}00)$ are shown in the WH plot in Fig. 3(b) together with the insensitive reflections $(3\bar{3}00)$ for the three *a*-plane InN films. In skew geometry both tilt and twist mosaics contribute to the broadening of the XRD ω scans, meaning they are contained in the derived slope angles $\Delta\omega$ (skew), while the intercept with the ordinate yielded the BPSF density for each sample. Summarized in Table I, we noted a drastic reduction in film mosaic tilt/twist (from ~3° to ~0.5°) and a decrease in BPSF densities (from $\sim 1.5\times10^{6}$ to $\sim 8\times10^{5}$ cm^{-1}) for the crossover from N-rich to In-rich growth. These values were also confirmed by transmission electron microscopy, highlighting the powerful nondestructive approach of the WH analysis.

Finally, the band gap energy was analyzed by photoluminescence (PL) and optical absorption at 300 K (Fig. 4). PL peak emission and band gap energies were independent of In/N ratio with values between 0.632–0.645 eV and $(0.70–0.71)\pm0.03$ eV, respectively. The ~70 meV redshift of the PL peak with respect to the band gap energy was comparable to that for the *m*-plane InN,[10] but larger than the typical Stokes shift of ~20–25 meV in *c*-plane InN.[13,14] This may be associated with the increased numbers of band-tail states in nonpolar InN due to the decoration of BPSFs by large point defect densities, mainly impurities.[25] The PL and band gap data are in good agreement with previous reports of *a*-plane InN (Refs. 5 and 26) and *c*-plane InN.[1,13,14]

The authors would like to thank C. Van de Walle for fruitful discussions and A. Hirai for the support with XRD analysis. This work was supported by AFOSR (D. J. Silversmith, program manager) and performed at the MRSEC facilities at UCSB (supported by NSF).

[1]H. Lu, W. J. Schaff, L. F. Eastman, J. Wu, W. Walukiewicz, V. Cimalla, and O. Ambacher, Appl. Phys. Lett. **82**, 1736 (2003).
[2]P. A. Anderson, C. H. Swartz, D. Carder, R. J. Reeves, S. M. Durbin, S. Chandril, and T. H. Myers, Appl. Phys. Lett. **89**, 184104 (2006).
[3]D. Segev and C. G. Van de Walle, Europhys. Lett. **76**, 305 (2006).
[4]C. L. Wu, H. M. Lee, C. T. Kuo, C. H. Chen, and S. Gwo, Phys. Rev. Lett. **101**, 106803 (2008).
[5]H. Lu, W. J. Schaff, L. F. Eastman, J. Wu, W. Walukiewicz, V. Cimalla, and O. Ambacher, Appl. Phys. Lett. **83**, 1136 (2003).
[6]P. D. C. King, T. D. Veal, C. F. McConville, F. Fuchs, J. Furthmüller, F. Bechstedt, P. Schley, R. Goldhahn, J. Schörmann, D. J. As, K. Lischka, D. Muto, H. Naoi, Y. Nanishi, H. Lu, and W. J. Schaff, Appl. Phys. Lett. **91**, 092101 (2007).
[7]E. Calleja, J. Grandal, M. A. Sanchez–Garcia, M. Niebelschütz, V. Cimalla, and O. Ambacher, Appl. Phys. Lett. **90**, 262110 (2007).
[8]Y. Kumagai, A. Tsuyuguchi, H. Naoi, T. Araki, H. Na, and Y. Nanishi, Phys. Status Solidi B **243**, 1468 (2006).
[9]X. L. Zhu, L. W. Guo, M. Z. Peng, B. H. Ge, J. Zhang, G. J. Ding, H. Q. Jia, H. Chen, and J. M. Zhou, J. Cryst. Growth **310**, 3726 (2008).
[10]G. Koblmüller, A. Hirai, F. Wu, C. S. Gallinat, G. D. Metcalfe, H. Shen, M. Wraback, and J. S. Speck, Appl. Phys. Lett. **93**, 171902 (2008).
[11]H. Okumura, K. Balakrishnan, H. Hamaguchi, T. Koizumi, S. Chichibu, H. Nakanishi, T. Nagatomo, and S. Yoshida, J. Cryst. Growth **189**, 364 (1998).
[12]G. Koblmüller, C. S. Gallinat, and J. S. Speck, J. Appl. Phys. **101**, 083516 (2007).
[13]C. S. Gallinat, G. Koblmüller, J. S. Brown, S. Bernardis, J. S. Speck, G. D. Chern, E. D. Readinger, H. Shen, and M. Wraback, Appl. Phys. Lett. **89**, 032109 (2006).
[14]G. Koblmüller, C. S. Gallinat, S. Bernardis, J. S. Speck, G. D. Chern, E. D. Readinger, H. Shen, and M. Wraback, Appl. Phys. Lett. **89**, 071902 (2006).
[15]B. A. Haskell, A. Chakraborty, H. Sasano, P. T. Fini, S. P. DenBaars, J. S. Speck, and S. Nakamura, J. Electron. Mater. **34**, 357 (2005).
[16]M. McLaurin, T. E. Mates, F. Wu, and J. S. Speck, J. Appl. Phys. **100**, 063707 (2006).
[17]A. Hirai, B. A. Haskell, M. B. McLaurin, F. Wu, M. C. Schmidt, K. C. Kim, T. J. Baker, S. P. DenBaars, S. Nakamura, and J. S. Speck, Appl. Phys. Lett. **90**, 121119 (2007).
[18]M. D. Craven, S. H. Lim, F. Wu, J. S. Speck, and S. P. DenBaars, Appl. Phys. Lett. **81**, 469 (2002).
[19]L. Lymperakis and J. Neugebauer, Proceedings of the International Workshop on Nitride Semiconductors, Montreux, 2008 (unpublished).
[20]C. S. Gallinat, G. Koblmüller, and J. S. Speck, J. Appl. Phys. **102**, 064907 (2007).
[21]T. Metzger, R. Höpler, E. Born, O. Ambacher, M. Stutzmann, R. Stömmer, M. Schuster, H. Göbel, S. Christiansen, M. Albrecht, and H. P. Strunk, Philos. Mag. A **77**, 1013 (1998).
[22]M. B. McLaurin, A. Hirai, E. Young, F. Wu, and J. S. Speck, Jpn. J. Appl. Phys. **47**, 5429 (2008).
[23]M. D. Craven, F. Wu, A. Chakraborty, B. Imer, S. P. DenBaars, and J. S. Speck, Appl. Phys. Lett. **84**, 1281 (2004).
[24]A. Hirai, F. Wu, and J. S. Speck (unpublished).
[25]P. Paskov, R. Schifano, B. Monemar, T. Paskova, S. Figge, and H. Hommel, J. Appl. Phys. **98**, 093519 (2005).
[26]F. Shikata, S. Hirano, T. Inoue, M. Orihara, Y. Hijikata, H. Yaguchi, and S. Yoshida, J. Cryst. Growth **301**, 517 (2007).